

LINEAR THEORY FOR SINGLE AND DOUBLE FLAP WAVEMAKERS

W.M. KUSUMAWINAHYU, N. KARJANTO AND G. KLOPMAN

Abstract. In this paper, we are concerned with deterministic wave generation in a hydrodynamic laboratory. A linear wavemaker theory is developed based on the fully dispersive water wave equations. The governing field equation is the Laplace equation for potential flow with several boundary conditions: the dynamic and kinematic boundary condition at the free surface, the lateral boundary condition at the wavemaker and the bottom boundary condition. In this work, we consider both single-flap and double-flap wavemakers. The velocity potential and surface wave elevation are derived, and the relation between the propagating wave height and wavemaker stroke is formulated. This formulation is then used to find how to operate the wavemaker in an efficient way to generate the desired propagating waves with minimal disturbances near the wavemaker.

1. INTRODUCTION

A wave tank in a hydrodynamic laboratory is a facility where maritime structures and ships can be tested by unidirectional waves on a model scale. It usually has a wavemaker at one side and a wave-absorbing beach at the other side. Generally, there are two types of wavemaker which are widely used in hydrodynamic laboratories, namely piston and flap type wavemakers, as shown in Figure 1 and 2. In this paper, we will consider specifically the flap type of wavemaker which is the preferred type for testing ships and structures in deep water. Here deep water means water depth which exceeds approximately a third of the wavelength. As an example, the Indonesian Hydrodynamic Laboratory (IHL) in Surabaya, East Java, Indonesia, uses single and double-flap wavemakers. Flap type wavemakers are moving partitions which rotate around one or more horizontal axes: single-flap wavemakers rotate about one hinge elevation, and double-flap wavemakers have

Received 15 March 2005, Accepted 27 July 2005.

2000 Mathematics Subject Classification: 76B15.

Key words and Phrases: linear theory, wavemaker, single-flap, double-flap, potential function, surface wave elevation, critical frequency, figure of merit.

two degrees of freedom. In order to gain basic insight, we first consider the single flap and then proceed to the double flap.

For the single-flap wavemaker, suppose that the wave tank has a still-water depth h and the flap hinge is located at a distance d below the still-water level. Although the hinge can be located above or at the bottom or even below the bottom, we will consider the first case. The bottom of the tank is taken to be flat and horizontal as well as impermeable. It is assumed that the flap moves with a monochromatic frequency and can reach a certain maximum stroke. The generated wave propagates towards the beach, which is considered to be perfectly absorbing, i.e. no wave is reflected. The aim is to find out the relation between the stroke of the wavemaker and the wave height far from the wavemaker. For this purpose, we need to know the velocity potential and the surface wave elevation which satisfy the governing equations for the wave tank. Further, the generation of irregular waves is considered.

In the case of a double-flap wavemaker, there are two actuators which move the lower flap (often called the main flap) and the upper flap. Since we use linear theory, the motion of a double-flap wavemaker can be regarded as the superposition of two single flaps. Thus the generated wave is the superposition of the waves produced by each single flap individually. Once the relation between the flap motions and the generated waves is determined, we know how to move the flap in order to generate a certain wave for testing a ship. The prescribed surface waves can also be irregular waves having two or many frequencies. Again, linear superposition can be used to sum solutions with different frequencies. Normally, the upper flap is used for the high frequencies, while the main flap is operated to generate the low-frequency waves. Then one needs to determine the critical frequency to decide for which frequency range the waves can be generated more efficiently by either the upper flap or the lower one. A customary way to find this critical frequency is through the use of the *Figure of Merit* (FoM), often also called *merit function*. As a function of frequency ω , the FoM describes the ratio between the free surface amplitude at the wavemaker, $x = 0$, and the one at infinity for a monochromatic motion of the wavemaker at frequency ω .

In the next section we will discuss the single-flap wavemaker theory. It starts with the simplest theory from Galvin [3] and then proceeds with the full linear theory for water waves, with the Laplace equation as governing equation and the appropriate boundary conditions. Section 3 will explore the double-flap wavemaker motion, using the theory for a single-flap obtained in Section 2. The *direct problem*, when the outcome is the generated wave for a prescribed flap movement, is presented first. Then we will discuss the *inverse problem*, where the objective is to determine the motion of the wavemaker in order to generate the desired surface wave. In that section we also determine the critical frequency as a criterium to decide whether to use the main flap or the upper flap. Further, the generation of irregular waves with a double-flap wavemaker is discussed. Finally, in Section 4 we will give some conclusions and recommendations for possible future research on this topic.

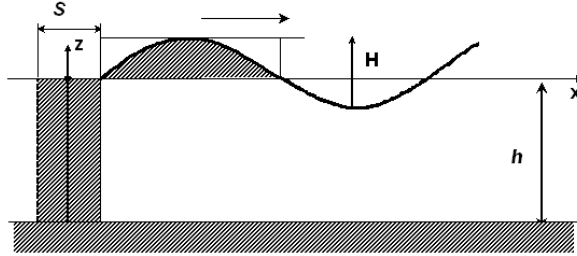


Figure 1: Sketch of a two-dimensional wave tank with piston-type of wavemaker.

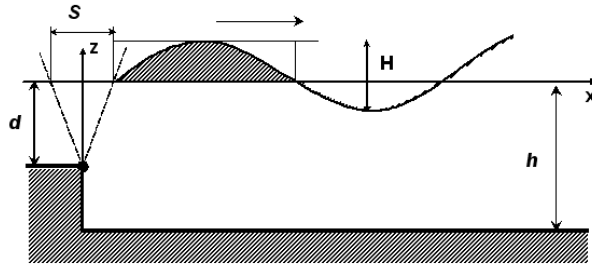


Figure 2: Sketch of a two-dimensional wave tank with single-flap wavemaker. The hinge is located at d below the still-water level.

2. SINGLE-FLAP WAVEMAKER THEORY

In this section, we will derive the simple shallow-water wavemaker theory of Galvin [3]. After that, the linear theory based on the full equations for water wave motion is discussed in more detail. By finding the ratio between the wave height and the wavemaker stroke, we solve the direct problem and the inverse problem at the same time. With the direct problem we mean that by prescribing the wavemaker stroke, the wave height far from the wavemaker follows as an outcome. The inverse problem is that if we desire to make a certain wave height far away from the wavemaker, we can calculate the stroke needed as an input to the wavemaker.

2.1 Galvin's theory for linear shallow-water waves

Consider a flap type wavemaker as shown at Figure 2. Galvin [3] proposed a simple theory for the generation of waves by this wavemaker, valid in shallow-water. Shallow-water means wavelengths L much larger than the water depth h ,

say $L > 10h$. He reasons that the water displaced by a full stroke of the wavemaker should be equal to the crest volume of the propagating wave. For a flap type of wavemaker with a maximum stroke S at the still-water level and a hinge depth d , the volume of water displaced during a whole stroke is $\frac{1}{2}Sd$. The volume of water in a wave crest for a wave with height H and wave number $k = \frac{2\pi}{L}$, is given by

$$\int_0^{L/2} \frac{1}{2}H \sin kx \, dx = \frac{1}{2} \frac{H}{k} \left(1 - \cos \frac{1}{2}kL \right) = \frac{H}{k}.$$

By equating the two volumes, we obtain the ratio of wave height H and the stroke S , given by

$$\left(\frac{H}{S} \right)_{\text{Galvin}} = \frac{1}{2}kd. \quad (1)$$

However, since our main objective is deep-water waves, Galvin's theory is not of direct use for our applications. But it can be used to check the asymptotic behaviour of our results for $kh \ll 1$.

2.2 Linear theory for arbitrary water depth

Let us start with the mass conservation equation for an *inviscid* fluid, with mass density ρ and velocity vector \mathbf{u} :

$$\frac{\partial \rho}{\partial t} + \nabla \cdot (\rho \mathbf{u}) = 0.$$

The fluid is assumed to be *incompressible* and ρ is taken a constant. Then, the mass conservation equation takes the simple form $\nabla \cdot \mathbf{u} = 0$, which is also known as the *continuity equation*. Furthermore, to good approximation for water waves, the motion may be taken to be *irrotational*, which physically means that individual fluid particles do not rotate. Mathematically, this implies that the vorticity vanishes, $\nabla \times \mathbf{u} = \mathbf{0}$. Then, there exists a single-valued velocity potential Φ such that $\mathbf{u} = \nabla \Phi$. By combining these two assumptions (incompressibility and irrotationality), we get the *Laplace equation* $\nabla^2 \Phi = 0$ as a governing equation for the water wave motion. For our wavemaker problem, it reads

$$\frac{\partial^2 \Phi}{\partial x^2} + \frac{\partial^2 \Phi}{\partial z^2} = 0, \quad -h \leq z \leq \eta(x, t), \quad x \geq s(z, t).$$

The boundary conditions are as follows

- the bottom boundary condition:

$$\frac{\partial \Phi}{\partial z} = 0, \quad \text{at } z = -h;$$

- the free-surface kinematic boundary condition

$$\frac{\partial \eta}{\partial t} + \frac{\partial \Phi}{\partial x} \frac{\partial \eta}{\partial x} = \frac{\partial \Phi}{\partial z}, \quad \text{at } z = \eta(x, t);$$

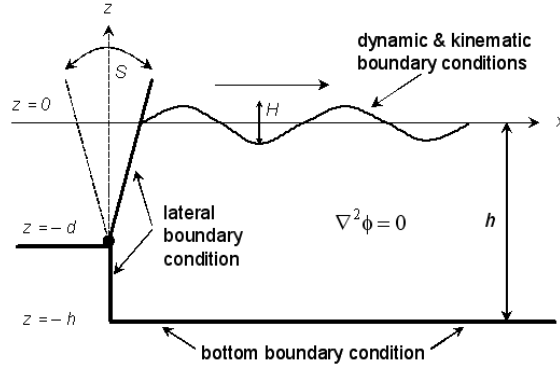


Figure 3: The single-flap wavemaker with the governing equation and its boundary conditions.

- the free-surface dynamic boundary condition

$$g\eta + \frac{\partial \Phi}{\partial t} + \frac{1}{2} \left[\left(\frac{\partial \Phi}{\partial x} \right)^2 + \left(\frac{\partial \Phi}{\partial z} \right)^2 \right] = 0, \quad \text{at } z = \eta(x, t);$$

- the lateral boundary condition at the wavemaker

$$\frac{\partial \Phi}{\partial z} \frac{\partial s}{\partial z} + \frac{\partial s}{\partial t} = \frac{\partial \Phi}{\partial x}, \quad \text{at } x = s(z, t).$$

Therefore we have a boundary value problem. Figure 3 illustrates the governing equation and its boundary conditions for a single-flap wavemaker.

Except for the bottom boundary condition, all boundary conditions are non-linear. Generally, it is hard to find the exact solution for this boundary value problem. The solution will be approximated by linearizing the nonlinear boundary conditions. The linearized equation model for our boundary value problem now reads

$$\begin{aligned} \frac{\partial^2 \Phi}{\partial x^2} + \frac{\partial^2 \Phi}{\partial z^2} &= 0, & -h \leq z \leq 0, \\ \frac{\partial \Phi}{\partial z} &= 0, & \text{at } z = -h; \\ \frac{\partial \eta}{\partial t} &= \frac{\partial \Phi}{\partial z}, & \text{at } z = 0; \\ \eta + \frac{1}{g} \frac{\partial \Phi}{\partial t} &= 0, & \text{at } z = 0; \\ \frac{\partial \Phi}{\partial x} &= \frac{\partial s(z, t)}{\partial t}, & \text{at } x = 0. \end{aligned} \quad (2)$$

(2)

(3)

The lateral boundary motion $s(z, t)$ for a single-flap wavemaker and sinusoidal flap motion becomes:

$$s(z, t) = \frac{1}{2}S(z) \sin(\omega t + \psi) = \begin{cases} \frac{1}{2}S \left(1 + \frac{z}{d}\right) \sin(\omega t + \psi) & , -d \leq z \leq 0; \\ 0 & , -h \leq z \leq -d, \end{cases}$$

which describes the wavemaker motion with maximum stroke S , wavemaker frequency ω and phase ψ .

2.3 Velocity potential and wave height-stroke relationship

The general solution for the Laplace equation with the bottom and the free-surface boundary conditions can be determined using the method of separation of variables; and is given by

$$\begin{aligned} \Phi(x, z, t) &= \frac{g}{\omega} \left[A \frac{\cosh k(h+z)}{\cosh kh} \sin(kx - \omega t - \psi) \right] \\ &+ \frac{g}{\omega} \left[C e^{-\kappa x} \frac{\cos \kappa(h+z)}{\cos \kappa h} \cos(\omega t + \psi) \right]. \end{aligned}$$

The first term is associated with a *progressive wave* (also called *propagating mode*), while the second term is associated with a spatially decaying *standing wave* and is often called an *evanescent mode*. The wave number k of a progressive wave and the wave number κ of an evanescent mode are related to the frequency ω by the *linear dispersion relation*

$$\omega^2 = gk \tanh kh \quad (4)$$

and

$$\omega^2 = -g\kappa \tan \kappa h. \quad (5)$$

By rewriting equation (4) and (5) as

$$\frac{\sigma^2}{kh} = \tanh kh$$

and

$$\frac{\sigma^2}{\kappa h} = -\tan \kappa h,$$

where $\sigma = \sqrt{\frac{\omega^2 h}{g}}$ is the non-dimensional frequency, it is easy to make plots of the solutions of these equations. The respective plots for $\sigma = 1$ are given in Figure 4.

Since there is an infinite number of solutions to equation (5), the solution for the boundary value problem has to be written as

$$\begin{aligned} \Phi(x, z, t) &= \frac{g}{\omega} \left[A \frac{\cosh k(h+z)}{\cosh kh} \sin(kx - \omega t - \psi) \right] \\ &+ \frac{g}{\omega} \left[\sum_{n=1}^{\infty} C^{[n]} e^{-\kappa^{[n]} x} \frac{\cos \kappa^{[n]}(h+z)}{\cos \kappa^{[n]} h} \cos(\omega t + \psi) \right], \end{aligned}$$

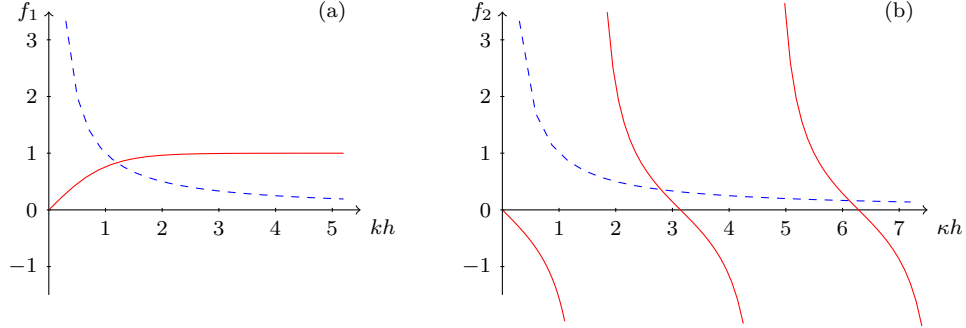


Figure 4: (a) Graphical representation of the linear dispersion relation for the propagating modes, the dash-dot curve represents the plot of $\frac{\sigma^2}{kh}$ while the solid one represents $\tanh kh$. (b) Graphical representation of the linear dispersion relation for the evanescent modes, showing four of the infinite numbers of roots. The dash-dot curve represents the plot of $\frac{\sigma^2}{kh}$, while the solid ones represent $-\tan \kappa h$.

where A and $C^{[n]}$ need to be determined. We assume all wave motion to originate from the wavemaker, so we only consider the positive $k > 0$ and $\kappa^{[n]} > 0$ to the dispersion relation (4) and (5). Note that the evanescent modes with amplitudes $C^{[n]}$, $n = 1, 2, \dots$ decay to zero far away from the wavemaker. Substitute this velocity potential into the linearized lateral boundary condition (3) to get

$$\begin{aligned} & \frac{g}{\omega} \left[\frac{Ak}{\cosh kh} \cosh k(h+z) - \sum_{n=1}^{\infty} \frac{C^{[n]} \kappa^{[n]}}{\cos \kappa^{[n]} h} \cos \kappa^{[n]}(h+z) \right] \\ & = \begin{cases} \frac{1}{2} S \omega \left(1 + \frac{z}{d}\right) & , -d \leq z \leq 0; \\ 0 & , -h \leq z \leq -d, \end{cases} \end{aligned} \quad (6)$$

which has to be valid for any $-h \leq z \leq 0$.

It is known from the Sturm-Liouville condition that the set

$$\left\{ \cosh k(h+z), \cos \kappa^{[n]}(h+z), n = 1, 2, \dots \right\}$$

forms an orthogonal set, namely

$$\int_{-h}^0 \cosh k(h+z) \cos \kappa^{[n]}(h+z) dz = 0$$

and

$$\int_{-h}^0 \cos \kappa^{[n]}(h+z) \cos \kappa^{[m]}(h+z) dz = 0, \quad m \neq n,$$

can be shown to hold because of the linear dispersion relationship (4) and (5).

Therefore, to find A both sides of (6) are multiplied by $\cosh k(h+z)$ and then integrated over the depth. Due to the orthogonality property, the evanescent terms containing $C^{[n]}$ are eliminated, and thus

$$\begin{aligned} A &= \frac{\sinh kh \int_{-d}^0 \frac{1}{2} \left(1 + \frac{z}{d}\right) \cosh k(h+z) dz}{2 \int_{-h}^0 \cosh^2(k(h+z)) dz} S \\ &= 2 \left(\frac{\sinh kh}{kd} \right) \frac{\cosh k(h-d) + kd \sinh kh - \cosh kh}{2kh + \sinh 2kh} S. \end{aligned} \quad (7)$$

To find $C^{[n]}$, multiply equation (6) by $\cos \kappa^{[n]}(h+z)$ and then integrate over the depth. It is found that

$$\begin{aligned} C^{[n]} &= \frac{\sin \kappa^{[n]} h \int_{-h}^0 \frac{1}{2} \left(1 + \frac{z}{d}\right) \cos \kappa^{[n]}(h+z) dz}{2 \int_{-h}^0 \cos^2(\kappa^{[n]}(h+z)) dz} S \\ &= -2 \left(\frac{\sin \kappa^{[n]} h}{\kappa^{[n]} d} \right) \frac{\cos \kappa^{[n]}(h-d) - \kappa^{[n]} d \sin \kappa^{[n]} h - \cos \kappa^{[n]} h}{2\kappa^{[n]} h + \sin 2\kappa^{[n]} h} S. \end{aligned} \quad (8)$$

Finally, the elevation of the generated surface wave $\eta(x, t)$ is readily found by applying the linearized dynamic boundary condition at the still-water level, equation (2), namely

$$\begin{aligned} \eta = -\frac{1}{g} \frac{\partial \Phi}{\partial t} \Big|_{z=0} &= A \cos(kx - \omega t - \psi) + \sum_{n=1}^{\infty} C^{[n]} e^{-\kappa^{[n]} x} \sin(\omega t + \psi) \\ &= \frac{H}{2} \cos(kx - \omega t - \psi) + \sum_{n=1}^{\infty} C^{[n]} e^{-\kappa^{[n]} x} \sin(\omega t + \psi), \end{aligned}$$

so A is the progressive amplitude and $H = 2A$ is the wave height.

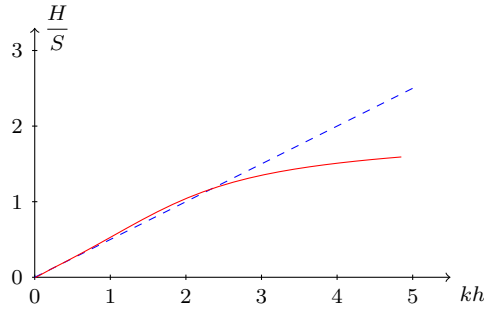


Figure 5: Wave height to stroke ratio H/S as a function of kh for a flap type wavemaker, with $d = h$, based on Galvin's theory, equation (1), (dash-dot curve), and the full linear theory, equation (10), (solid curve).

The wave height of the progressive wave is determined by evaluating $\eta(x, t)$ far from wavemaker, where the evanescent modes vanish, namely

$$\eta = \frac{H}{2} \cos(kx - \omega t - \psi), \quad \kappa^{[1]}x \gg 1.$$

Since the relation between A and S is known, the ratio of the wave height $H = 2A$ and the stroke S is given by

$$\left(\frac{H}{S}\right)_{\text{linear}} = 4 \left(\frac{\sinh kh}{kd}\right) \frac{\cosh k(h-d) + kd \sinh kh - \cosh kh}{2kh + \sinh 2kh}. \quad (9)$$

When the hinge of the flap is located at the bottom of the wave tank we have $d = h$ and the ratio becomes

$$\left(\frac{H}{S}\right)_{\text{linear}} = 4 \left(\frac{\sinh kh}{kh}\right) \frac{1 + kh \sinh kh - \cosh kh}{2kh + \sinh 2kh}, \quad (10)$$

as also found in Dean and Dalrymple [2] and Gilbert et al [4]. Figure 5 shows the plots of wave height to stroke ratio for flap type of wavemaker using the full linear theory, equation (10), compared to Galvin's theory, equation (1), when $d = h$. Therefore Galvin's simple theory gives a good approximation to the wave height to stroke ratio for small kh .

The wave height to stroke ratio (9) gives the transformation from the stroke of the single-flap wavemaker motion to the progressive wave height generated by that wavemaker motion. For the testing of ships in a hydrodynamic laboratory, normally the wave height H of a monochromatic signal is specified. Using (9), we now can determine the required stroke of the wavemaker.

Often, the desired waves are not regular but irregular. These waves can be represented as a summation of several monochromatic waves, namely

$$\eta(x, t) = \sum_{i=1}^N \frac{1}{2} H_i \cos(k_i x - \omega_i t - \psi_i), \quad (11)$$

where each wave number - frequency pair (k_i, ω_i) satisfies the linear dispersion relation (4). Since we consider linear wavemaker theory the wavemaker has to be moved with the flap motion

$$s(z, t) = \begin{cases} \frac{1}{2} \left(1 + \frac{z}{d}\right) \sum_{i=1}^N S_i \sin(\omega_i t + \psi_i) & , -d \leq z \leq 0; \\ 0 & , -h \leq z \leq -d, \end{cases}$$

where every S_i satisfies the wave height to stroke ratio (9) associated with the corresponding wave height H_i .

3. DOUBLE-FLAP WAVEMAKER THEORY

This section is started by the formulation of the double-flap wavemaker motion and the surface waves generated by the flap movement. This formulation is referred to as the direct problem. Once the relation between the flap strokes and the height of the generated progressive wave is found we proceed with the inverse problem. There, the desired surface wave at a position far from the wavemaker is given, generally in the form of an irregular wave. Hence it can be represented as a summation of a finite number of regular waves with different frequencies and amplitudes. Regular waves with high frequencies are generated by moving the upper flap, while the low-frequency waves are generated by the main flap. Thus we need to find the critical frequency that separates the frequency range for which one shall operate either the upper flap or the main flap.

3.1 The generated surface waves

Consider a wave tank with a double-flap wavemaker at one side and a wave-absorbing beach at the other side, as shown in Figure 6. Suppose that the depth of the tank is h and the hinges of the upper flap and main flap are located at distances d_1 and d_2 respectively below the still-water level. If the upper flap moves with frequency ω_1 and has a maximum stroke S_1 and the main flap moves with frequency ω_2 and has a maximum stroke S_2 , then we can distinguish three cases for the motion of the wavemaker: upper flap motion, main flap motion, and combined flap motion. Figure 7 illustrates these three situations. Since we consider only the linear theory of wavemakers, then the last case is just the superposition of the two preceding cases.

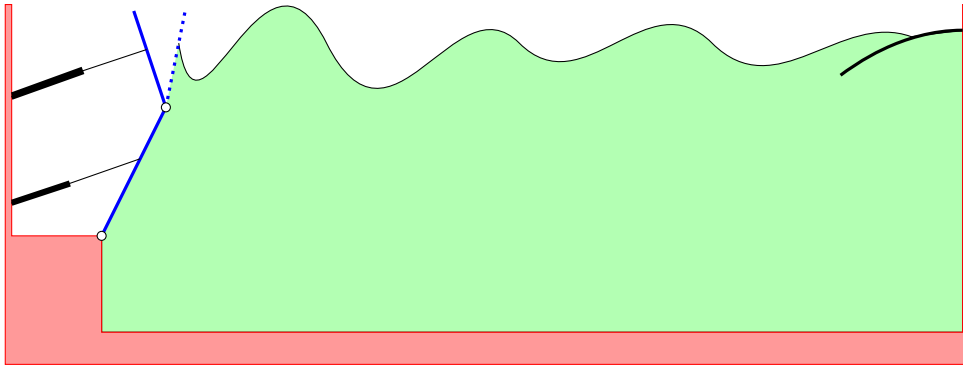


Figure 6: Schematic figure of a double-flap wavemaker structure.

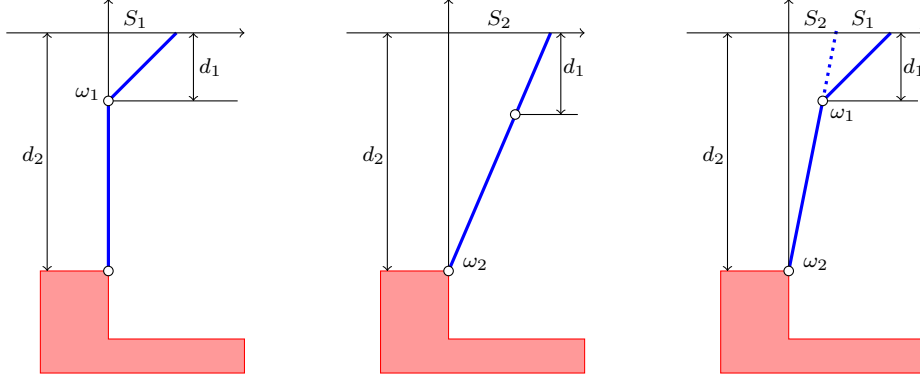


Figure 7: Illustration of three cases in the double flaps wavemaker: upper flap motion (left), main flap motion (middle), combination of upper and main flap (right).

The cases when only the upper flap moves with stroke S_1 or the main flap with stroke S_2 has been treated in the previous section on single-flap motion. Here, we will discuss the case of both flaps moving simultaneously, the upper flap with frequency ω_1 and the main flap with frequency ω_2 .

The horizontal displacement $s(z, t)$ when both the upper flap and the main flap move together is given by

$$s(z, t) = \begin{cases} \frac{1}{2} \left[S_1 \left(1 + \frac{z}{d_1} \right) \sin(\omega_1 t + \psi_1) + S_2 \left(1 + \frac{z}{d_2} \right) \sin(\omega_2 t + \psi_2) \right] & , -d_1 \leq z \leq 0; \\ \frac{1}{2} S_2 \left(1 + \frac{z}{d_2} \right) \sin(\omega_2 t + \psi_2) & , -d_2 \leq z \leq -d_1; \\ 0 & , -h \leq z \leq -d_2. \end{cases}$$

By linear superposition, the corresponding velocity potential Φ for this condition is the sum of the velocity potentials Φ_1 and Φ_2 , namely

$$\begin{aligned} \Phi(x, z, t) &= \frac{g}{\omega_1} \left[A_1 \frac{\cosh k_1(z+h)}{\cosh k_1 h} \sin(k_1 x - \omega_1 t - \psi_1) \right] \\ &+ \frac{g}{\omega_1} \left[\sum_{n=1}^{\infty} C_1^{[n]} e^{-\kappa_1^{[n]} x} \frac{\cos \kappa_1^{[n]}(z+h)}{\cos \kappa_1^{[n]} h} \cos(\omega_1 t + \psi_1) \right] \\ &+ \frac{g}{\omega_2} \left[A_2 \frac{\cosh k_2(z+h)}{\cosh k_2 h} \sin(k_2 x - \omega_2 t - \psi_2) \right] \\ &+ \frac{g}{\omega_2} \left[\sum_{n=1}^{\infty} C_2^{[n]} e^{-\kappa_2^{[n]} x} \frac{\cos \kappa_2^{[n]}(z+h)}{\cos \kappa_2^{[n]} h} \cos(\omega_2 t + \psi_2) \right], \end{aligned}$$

where the coefficients A_1 , A_2 , $C_1^{[n]}$, and $C_2^{[n]}$ are as given for the single-flap case. The

surface elevation $\eta(x, t)$ produced by the double-flap wavemaker becomes, according to the linearized dynamic boundary condition (2):

$$\begin{aligned}\eta(x, t) &= -\frac{1}{g} \frac{\partial \Phi}{\partial t} \Big|_{z=0} \\ &= A_1 \cos(k_1 x - \omega_1 t - \psi_1) + \sum_{n=1}^{\infty} C_1^{[n]} e^{-\kappa_1^{[n]} x} \sin(\omega_1 t + \psi_1) \\ &+ A_2 \cos(k_2 x - \omega_2 t - \psi_2) + \sum_{n=1}^{\infty} C_2^{[n]} e^{-\kappa_2^{[n]} x} \sin(\omega_2 t + \psi_2).\end{aligned}$$

The generated progressive wave is determined by evaluating $\eta(x, t)$ far from wavemaker, where the evanescent modes vanish:

$$\begin{aligned}\eta(x, t) &= A_1 \cos(k_1 x - \omega_1 t - \psi_1) + A_2 \cos(k_2 x - \omega_2 t - \psi_2) \\ &= \frac{H_1}{2} \cos(k_1 x - \omega_1 t - \psi_1) + \frac{H_2}{2} \cos(k_2 x - \omega_2 t - \psi_2),\end{aligned}$$

where

$$H_1 = 4 \left(\frac{\sinh k_1 h}{k_1 d_1} \right) \frac{\cosh k_1 (h - d_1) + k_1 d_1 \sinh k_1 h - \cosh k_1 h}{2k_1 h + \sinh 2k_1 h} S_1,$$

and

$$H_2 = 4 \left(\frac{\sinh k_2 h}{k_2 d_2} \right) \frac{\cosh k_2 (h - d_2) + k_2 d_2 \sinh k_2 h - \cosh k_2 h}{2k_2 h + \sinh 2k_2 h} S_2,$$

relate the wave heights H_1 and H_2 to the strokes S_1 and S_2 , respectively. Note, that for the case $\omega_1 \neq \omega_2$, the maximum wave height is $H_1 + H_2$ and the minimum wave height is $|H_1 - H_2|$ in the generated bi-chromatic wave pattern.

3.2 Inverse Problem

In the previous subsection, the formulations give the heights of the generated waves for a prescribed flap motion. The wave heights are expressed in terms of the wavemaker stroke, the hinge positions, water depth and the frequencies of the flap motion. In this subsection we want to determine how to move the flaps in such a way such that the desired waves are generated. Normally, the upper flap generates the high-frequency waves, while the main flap generates the low-frequency ones. Generally, the desired waves are not regular waves and are written as a linear superposition of many regular waves with various frequencies. Hence one needs to find the critical frequency above which one uses the upper flap and below which one uses the main flap to generate waves. For this reason, the next subsection will discuss a method to determine the critical frequency.

3.2.1 The critical frequency

A *merit* function, also known as a *Figure-of-Merit* function, is a function that measures the agreement between data and a model fitted with for a particular choice of the parameters. By convention, the merit function is small when the agreement is good. In the process known as regression, parameters are adjusted based on the value of the merit function until a minimum is obtained, thus producing a best-fit. The corresponding parameters, giving the smallest value of the merit function, are known as the best-fit parameters (Press [5]).

Our aim is to determine for which frequency range the upper flap and the main flap will be used. Therefore, we need a method to solve this problem. We introduce the Figure of Merit (FoM) of a wavemaker flap, which is given by the ratio of the surface wave amplitude at the wavemaker and the one far from the wavemaker. It reads (Dalzell [1]):

$$\text{FoM}(\omega) = \frac{\sqrt{A^2(\omega) + \left[\sum_{n=1}^{\infty} C^{[n]}(\omega)\right]^2}}{A(\omega)},$$

where A is the propagating mode amplitude and $C^{[n]}$ are the evanescent mode amplitudes. Note that the FoM is always larger or equal to one. The ideal case is if the FoM equals one. Then there are no evanescent modes, which is desirable since the increased wave height near the wavemaker, due to the presence of the evanescent modes, may for instance trigger undesirable wave breaking near the wavemaker. Let the FoM of the upper flap be denoted by FoM_1 and the FoM of the main flap be denoted by FoM_2 , then there exists a critical frequency ω^* such that $\text{FoM}_1(\omega^*) = \text{FoM}_2(\omega^*)$. The plots of $\text{FoM}_1(\omega^*)$ and $\text{FoM}_2(\omega^*)$ can easily be drawn when we have found the progressive wavenumber k and evanescent wave numbers $\kappa^{[n]}$ corresponding to a certain range of ω by solving the *linear dispersion relation* (4) and (5).

For low frequencies the upper flap $\text{FoM}_1(\omega)$ will be higher than the main flap $\text{FoM}_2(\omega)$, and above a critical frequency ω^* , it will be just opposite. The critical frequency is obtained where the plotted lines of the FoM cross each other. Accordingly, for $0 < \omega \leq \omega^*$, the main flap is used, and for $\omega > \omega^*$, the upper flap is used.

The following derivation shows that the determination of the critical frequency depends only on the configuration of wavemaker, namely the wave tank depth h and the location of the hinges d_1 as well as d_2 below the still-water level. Starting from $\text{FoM}_1(\omega^*) = \text{FoM}_2(\omega^*)$ and taking the square of both sides, we obtain

$$\begin{aligned} \frac{A_1^2(\omega^*) + \left[\sum_{n=1}^{\infty} C_1^{[n]}(\omega^*)\right]^2}{A_1^2(\omega^*)} &= \frac{A_2^2(\omega^*) + \left[\sum_{n=1}^{\infty} C_2^{[n]}(\omega^*)\right]^2}{A_2^2(\omega^*)}, \text{ or} \\ 1 + \left[\frac{\sum_{n=1}^{\infty} C_1^{[n]}(\omega^*)}{A_1(\omega^*)}\right]^2 &= 1 + \left[\frac{\sum_{n=1}^{\infty} C_2^{[n]}(\omega^*)}{A_2(\omega^*)}\right]^2. \end{aligned}$$

By re-arranging the terms and taking the square root of both sides, we get

$$\frac{A_1(\omega^*)}{A_2(\omega^*)} = \pm \frac{\sum_{n=1}^{\infty} C_1^{[n]}(\omega^*)}{\sum_{n=1}^{\infty} C_2^{[n]}(\omega^*)}, \quad (12)$$

where $A_1(\omega^*)$, $A_2(\omega^*)$, $C_1^{[n]}(\omega^*)$, and $C_2^{[n]}(\omega^*)$ are related to S_1 and S_2 through (7) and (8):

$$\begin{aligned} A_1(\omega^*) &= 2 \left(\frac{S_1 \sinh k^* h}{k^* d_1} \right) \frac{\cosh k^*(h - d_1) + k^* d_1 \sinh(k^* h) - \cosh(k^* h)}{2k^* h + \sinh(2k^* h)}, \\ A_2(\omega^*) &= 2 \left(\frac{S_2 \sinh k^* h}{k^* d_2} \right) \frac{\cosh k^*(h - d_2) + k^* d_2 \sinh(k^* h) - \cosh(k^* h)}{2k^* h + \sinh(2k^* h)}, \\ C_1^{[n]}(\omega^*) &= -2 \left(\frac{S_1 \sin \kappa_*^{[n]} h}{\kappa_*^{[n]} d_1} \right) \frac{\cos \kappa_*^{[n]}(h - d_1) - \kappa_*^{[n]} d_1 \sin(\kappa_*^{[n]} h) - \cos(\kappa_*^{[n]} h)}{2\kappa_*^{[n]} h + \sin(2\kappa_*^{[n]} h)}, \\ C_2^{[n]}(\omega^*) &= -2 \left(\frac{S_2 \sin \kappa_*^{[n]} h}{\kappa_*^{[n]} d_2} \right) \frac{\cos \kappa_*^{[n]}(h - d_2) - \kappa_*^{[n]} d_2 \sin(\kappa_*^{[n]} h) - \cos(\kappa_*^{[n]} h)}{2\kappa_*^{[n]} h + \sin(2\kappa_*^{[n]} h)}. \end{aligned}$$

By substituting these quantities into (12), we have the following relation at $\omega = \omega^*$:

$$\begin{aligned} &\frac{\cosh k^*(h - d_1) + k^* d_1 \sinh(k^* h) - \cosh(k^* h)}{\cosh k^*(h - d_2) + k^* d_2 \sinh(k^* h) - \cosh(k^* h)} = \\ &\pm \frac{\sum_{n=1}^{\infty} \left[\cos \kappa_*^{[n]}(h - d_1) - \kappa_*^{[n]} d_1 \sin(\kappa_*^{[n]} h) - \cos(\kappa_*^{[n]} h) \right] / [\kappa_*^{[n]} (2\kappa_*^{[n]} h + \sin(2\kappa_*^{[n]} h))]}{\sum_{n=1}^{\infty} \left[\cos \kappa_*^{[n]}(h - d_2) - \kappa_*^{[n]} d_2 \sin(\kappa_*^{[n]} h) - \cos(\kappa_*^{[n]} h) \right] / [\kappa_*^{[n]} (2\kappa_*^{[n]} h + \sin(2\kappa_*^{[n]} h))]}, \quad (13) \end{aligned}$$

where k^* , $\kappa_*^{[n]}$, and ω^* satisfy the linear dispersion relation

$$(\omega^*)^2 = gk^* \tanh(k^* h) = -g\kappa_*^{[n]} \tan(\kappa_*^{[n]} h).$$

The configuration of the double-flap wavemaker in the towing tank of the IHL is: $h = 5.5$ m depth and the position of hinges is at $d_1 = 0.83$ m and $d_2 = 2.55$ m below the still-water level. For this configuration, we have drawn the plots of FoM₁ and FoM₂ in the frequency domain as well as in the wave period domain, as shown in Figure 8. It can be noticed that for the IHL towing tank configuration the critical frequency is $\omega^* = 3.7512$ rad/s, and the critical period is $T^* = 2\pi/\omega^* = 1.675$ sec. It can also be observed that at the critical point, the value of FoM₁ as well as FoM₂ are both very close to 1, the optimum value. Further it can be seen that if the main flap and upper flap are used in the appropriate frequency ranges, the FoM is less than 1.1 for $T > 0.7$ s (or $\omega < 9$ rad/s).

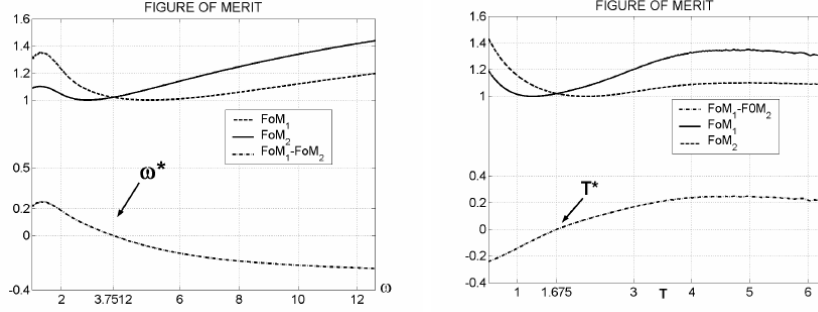


Figure 8: Graphs of the Figure of Merit as a function of frequency (left) and as a function of wave period (right), for $h = 5.5$ m, $d_1 = 0.83$ m, and $d_2 = 2.55$ m.

3.2.2 Irregular wave motion for the double-flap wavemaker

Let the desired irregular waves, to be generated by the double-flap wavemaker, be expressed by (11). In order to distinguish the wave components that have to be generated by the upper flap from the ones that will be generated by the main flap, the desired wave field needs to be separated into two parts:

$$\begin{aligned} \eta(x, t) &= \sum_{i=1}^{N_1} \frac{H_{1i}}{2} \cos(k_{1i}x - \omega_{1i}t - \psi_{1i}) + \sum_{i=1}^{N_2} \frac{H_{2i}}{2} \cos(k_{2i}x - \omega_{2i}t - \psi_{2i}) \\ &= \eta_H(x, t) + \eta_L(x, t), \end{aligned} \quad (14)$$

where $\omega_{1i} > \omega^*$ denote the frequencies of the wave components that need to be generated by the upper flap, while $0 < \omega_{2i} \leq \omega^*$ are the frequencies of the wave components which will be sent to the main flap. Subscripts H and L indicate high and low frequency, respectively.

Since we are concerned with linear theory, the flap motion is the superposition of the flap motion by the individual wave components. The motion of the double-flap wavemaker to generate the irregular wave field (14) becomes

$$x = \begin{cases} \frac{1}{2} \left(1 + \frac{z}{d_1} \right) \sum_{i=1}^{N_1} S_{1i} \sin(\omega_{1i}t + \psi_{1i}) \\ \quad + \frac{1}{2} \left(1 + \frac{z}{d_2} \right) \sum_{i=1}^{N_2} S_{2i} \sin(\omega_{2i}t + \psi_{2i}) & , -d_1 \leq z \leq 0; \\ \frac{1}{2} \left(1 + \frac{z}{d_2} \right) \sum_{i=1}^{N_2} S_{2i} \sin(\omega_{2i}t + \psi_{2i}) & , -d_2 \leq z \leq -d_1; \\ 0 & , -h \leq z \leq -d_2, \end{cases}$$

where

$$S_{1i} = \left(\frac{k_{1i}d_1}{4 \sinh k_{1i}h} \right) \frac{2k_{1i}h + \sinh 2k_{1i}h}{\cosh k_{1i}(h - d_1) + k_{1i}d_1 \sinh k_{1i}h - \cosh k_{1i}h} H_{1i},$$

$$S_{2i} = \left(\frac{k_{2i}d_2}{4 \sinh k_{2i}h} \right) \frac{2k_{2i}h + \sinh 2k_{2i}h}{\cosh k_{2i}(h - d_2) + k_{2i}d_2 \sinh k_{2i}h - \cosh k_{2i}h} H_{2i},$$

and k_{ji} satisfy the linear dispersion relation (4) with respect to ω_{ji} .

4. CONCLUDING REMARKS

In this paper, we consider a wave tank that has a wavemaker on one side and an absorbing beach on the other side. A linear theory for the flap type of wavemaker based on the full equation for linear water waves is presented. It has been discussed for both the single-flap and the double-flap wavemaker motion. By solving the governing equation with its corresponding boundary conditions, it turns out that the surface wave elevation contains a progressive wave part and an evanescent modes part, where the latter part vanishes far from the wavemaker. Furthermore, there is an explicit relation between the wave height of the generated surface wave elevation in the far field and the stroke of the wavemaker. This relation depends explicitly on the water depth, the hinge position, and the wave frequency.

Therefore, we are able to solve both the direct problem, where the wavemaker stroke is prescribed and the wave height is the outcome, as well as the inverse problem, where the wave height is given and the wavemaker stroke follows as a result. The latter case is more likely to be the desired situation for performing experiments in the laboratory, allowing one to control the wavemaker motion in such a way that the desired wave field is realized.

We also apply linear theory to the case when the wavemaker has double flaps. This type of the wavemaker is useful in generating waves in a wider range of frequencies. The double-flap wavemaker has two actuators that move the upper flap and the main flap. Normally, the upper flap is used to generate the wave components with a frequency higher than a certain critical frequency ω^* , while the main flap is used to generate the wave components with frequencies below ω^* . By applying the Figure of Merit (FoM) on the wavemaker flaps, one can determine the critical frequency ω^* , see equation (13). The FoM depends only on the wave tank depth and the position of the hinges. For a certain wave tank configuration, the critical frequency has to be determined. Hence, one can decide when to use either the upper flap or the main flap. Since the calculation is based on linear theory, linear superposition can be used to construct an irregular wave field.

This wavemaker theory can be extended using nonlinear theory. This will involve mode generation, as a consequence of nonlinear interaction among monochromatic wave components at a higher order. This nonlinear extension is expected to be executed in similar research in the future.

Acknowledgement. This work has been executed at the Industrial & Applied Mathematics R & D Group or Kelompok Penelitian dan Pengembangan Matematika Industri dan Terapan Institut Teknologi Bandung (KPP MIT - ITB), Indonesia and is supported by the Small Project Facility of the European Union Jakarta,

entitled ‘Building Academia-Industry Partnership in the Sectors of Marine and Telecommunication Technology’. The authors want to thank Dr. Andonowati and Prof. E. van Groesen for inviting them to participate in this project. Part of this work has been executed at the University of Twente, the Netherlands, under the project ‘Prediction and generation of deterministic extreme waves in hydrodynamic laboratories’ (TWI.5374) of the Netherlands Organization of Scientific Research NWO, subdivision Applied Sciences STW. The helpful discussions throughout the execution of this research with Dr. René Huijsmans are very much appreciated. The second author also wishes to thank MARIN, the Netherlands, for their support in the above mentioned STW project.

REFERENCES

1. J. F. DALZELL, “Analysis of Articulated Flap Wavemakers”, *Technical Report TR75 - 1, ABA Electromechanical Systems*, Pinellas Park, Florida, USA, March 1975.
2. R. G. DEAN AND R. A. DALRYMPLE, *Water Wave Mechanics for Engineers and Scientists*, volume **2** of Advanced Series on Ocean Engineering, World Scientific, Singapore, 1991.
3. C. J. GALVIN, JR, “Wave Height Prediction for Wave Generators in Shallow-Water”, *Tech Memo 4, U.S. Army, Coastal Engineering Research center*, March 1964.
4. G. GILBERT, D. M. THOMPSON & A. J. BREWER, “Design Curves for Regular and Random Wave Generators”, *J. Hydraulic Res.* **2**, no. 2, 163 – 196, 1971.
5. W. H. PRESS, B. P. FLANNERY, S. A. TEUKOLSKY, *Numerical Recipes in FORTRAN: The Art of Scientific Computing*, Cambridge University Press, Cambridge, 1992.

W.M. KUSUMAWINAHYU: Department of Mathematics, Institut Teknologi Bandung, Jl. Ganesha 10 Bandung 40132, Indonesia.
 Department of Mathematics, Universitas Brawijaya, Jl. May. Jend. Haryono 169 Malang 65145, Indonesia.
 E-mail: muharini@dns.math.itb.ac.id

N. KARJANTO: Applied Analysis and Mathematical Physics Group, Department of Applied Mathematics, University of Twente, P.O. Box 217, 7500 AE, Enschede, The Netherlands.
 E-mail: n.karjanto@math.utwente.nl

G. KLOPMAN: Applied Analysis and Mathematical Physics Group, Department of Applied Mathematics, University of Twente, P.O. Box 217, 7500 AE, Enschede, The Netherlands. Albatros Flow Research, Voorsterweg 28, 8316 PT, Marknesse, The Netherlands.
 E-mail: g.klopman@math.utwente.nl